Exploring Indoor White Spaces in Metropolises

XUHANG YING, University of Washington
JINCHENG ZHANG and LICHAO YAN, The Chinese University of Hong Kong
YU CHEN, University of California, San Diego
GUANGLIN ZHANG, Donghua University
MINGHUA CHEN, The Chinese University of Hong Kong
RANVEER CHANDRA, Microsoft Research, Redmond

It is a promising vision to exploit *white spaces*, that is, vacant VHF and UHF TV channels, to meet the rapidly growing demand for wireless data services in both outdoor and indoor scenarios. While most prior works have focused on outdoor white space, the indoor story is largely open for investigation. Motivated by this observation and discovering that 70% of the spectrum demand comes from indoor environment, we carry out a comprehensive study to explore *indoor* white spaces. We first conduct a large-scale measurement study and compare outdoor and indoor TV spectrum occupancy at 30+ diverse locations in a typical metropolis—Hong Kong. Our results show that abundant white spaces are available in different areas in Hong Kong, which account for more than 50% and 70% of the entire TV spectrum in outdoor and indoor scenarios, respectively. Although there are substantially more white spaces indoors than outdoors, there have been very few solutions for identifying indoor white space. To fill in this gap, we develop the first data-driven, low-cost indoor white space identification system for White-space Indoor Spectrum EnhanceR (WISER), to allow secondary users to identify white spaces for communication without sensing the spectrum themselves. We design the architecture and algorithms to address the inherent challenges. We build a WISER prototype and carry out real-world experiments to evaluate its performance. Our results show that WISER can identify 30%–40% more indoor white spaces with negligible false alarms, as compared to alternative baseline approaches.

CCS Concepts: • **Networks → Location based services**; **Wireless local area networks**; **Network performance analysis**;

Additional Key Words and Phrases: TV white spaces, clustering algorithms, sensor placement

This work was present in part at ACM Mobicom 2013 (Ying et al. 2013).
The work described in this article was partially supported by National Basic Research Program of China (Projects No. 2012CB315904 and No. 2013CB336700) and several grants from the University Grants Committee of the Hong Kong Special Administrative Region, China (Area of Excellence Grant Project No. AoE/E-02/08 and General Research Fund Projects No. 411010 and No. 411011).
Authors' addresses: X. Ying was with Department of Information Engineering at The Chinese University of Hong Kong when this work is done. He is now with Department of Electrical Engineering at University of Washington; email: xhying@uw.edu; J. Zhang, L. Yan, Y. Chen, and M. Chen are with Department of Information Engineering at The Chinese University of Hong Kong; emails: perfume0607@gmail.com, yanlichaonike@gmail.com, yuc388@eng.ucsd.edu, minghua@ie.cuhk.edu.hk; Guanglin Zhang was with Department of Information Engineering at The Chinese University of Hong Kong when this work is done. He is now with Department of Communication and Electronic Engineering at Donghua University; email: glzhang@dhu.edu.cn; R. Chandra is with Microsoft Research at Redmond; email: ranveer@microsoft.com.

https://doi.org/10.1145/3059149

ACM Reference format:
Xuhang Ying, Jincheng Zhang, Lichao Yan, Yu Chen, Guanglin Zhang, Minghua Chen, and Ranveer Chandra. 2017. Exploring Indoor White Spaces in Metropolises. *ACM Trans. Intell. Syst. Technol.* 9, 1, Article 9 (August 2017), 25 pages.
https://doi.org/10.1145/3059149

1 INTRODUCTION

The skyrocketing growth of mobile devices and mobile multimedia applications has translated into the demand for greater wireless capacity and consequently a need of extra available radio frequency (RF) spectrum. Since most RF spectrum has been licensed for different purposes (satellites, TV broadcasting, radio, radars, cellular services, etc.), a recent concept of Dynamic Spectrum Access (DSA) is being explored to enable more efficient use of the spectrum without interfering with existing licensed users and their devices.

A recent manifestation of DSA is in the TV spectrum. In 2008, the FCC passed a historic ruling that allowed unlicensed devices (i.e., secondary users) to access the locally unoccupied TV spectrum (also called TV white spaces or, simply, white spaces), without harmful interference to existing TV receivers (i.e., primary users). White space devices, similar to the Wi-Fi devices of today, are required to detect the available spectrum before using it for communication. Per a 2010 FCC Second Order and Report (FCC 2010), such devices can detect available spectrum either using spectrum sensing or by querying a geo-location web service over the Internet.

Currently, most white space devices and standards are being designed around querying the geo-location database for white space availability. This is primarily because spectrum sensing is expensive—in cost, energy consumption, and complexity of the circuitry. Furthermore, it is more difficult to accurately sense the presence of TV signals at low thresholds with commercial, off-the-shelf hardware. In contrast, the geo-location approach does not require any hardware and is easier to implement. Devices report their locations to a web service, which in turn returns a list of available TV channels for use at that location.[1] See Gibson (2010) for a survey on this line of research. However, this approach suffers from inherent inefficiency. The geo-location database determines available spectrum using empirical propagation models recommended by the FCC, which do *not* account for built environments, such as buildings and other man-made obstructions, especially in urban areas. In a measurement study in Yan and Chen (2011), an in-operation geo-location database service reports only half of vacant channels across a major city. As argued by Plets et al. (2009) and Asp et al. (2014), different building types and construction materials will introduce different penetration loss. This makes it very difficult to build a precise propagation model involving building penetration loss in a complicated metropolitan area. Considering that buildings significantly attenuate radio signals, the geo-location service is very conservative in detecting white space availability at a given location.

In this article, we carry out measurement-driven analysis and design for indoor white space networking. We first conduct a large-scale measurement campaign at 30+ diverse locations in a typical metropolis, which reveals that more than 50% and 70% of the TV spectrum are white spaces in outdoor and indoor scenarios, respectively. The study in König et al. (2014) shows that the duty cycles of indoor UHF TV channels are very small. Most bands only have a duty cycle less than 30%. A large amount of indoor white spaces exist in both frequency and time domains. While there are

[1]To avoid interference to white space users from wireless microphone usage, wireless microphone users are suggested to register the location and frequency usage to the geo-location database. In this way, the database can exclude the frequency occupied by wireless microphone at the location and within its estimated interfering neighbors from the returned list.

significantly more white spaces indoors than outdoors, there have been very few solutions for identifying indoor white spaces. Given that most people are indoors 80% of the time (Klepeis et al. 2001) and 70% of spectrum demand comes from indoor environments (Chandrasekhar et al. 2008), it will be extremely useful if it were possible to use the vacant TV channels indoors as efficiently as possible. There are a lot of works exploring TV white spaces recently. Bedogni et al. (2014) supports that short-range communication is possible through indoor white spaces and Zhang et al. (2015) designs an indoor white space network. Holland et al. (2015) carries out a series of experiments in TV white space and demonstrate good potential toward indoor deployment. These works provide us effective mechanisms to exploit unoccupied TV channels.

We therefore develop a system, called White-space Indoor Spectrum EnhanceR (WISER) to identify vacant TV channels for indoor white space networking, while (i) not requiring client devices to sense the spectrum, (ii) constructing more accurate local white space database by integrating outdoor and indoor spectrum data, and (iii) not interfering with TV transmissions.

WISER enables buildings to be "white space enabled" using an integrated approach of profiling, sensor placement, and integration with geo-location databases. It provides a technique for building owners or managers to get their building profiled for white space use, based on which WISER strategically determines a few locations to place RF sensors. These sensors capture the additionally available white space spectrum in the building. Ideally, we would require a very dense placement of RF sensors to obtain every additionally available channel. However, such approach can be very expensive due to the large number of RF sensors.[2] Hence, we propose a clustering scheme to reduce the number of sensors needed to (i) capture white space variations in indoor environments, yet (ii) provide most of the additional channels for indoor use.

Throughout this article, we make the following contributions:

In Section 3, using comprehensive measurements in Hong Kong, we show that more than 50% and 70% of the TV spectrum is white space in outdoor and indoor scenarios, respectively. Further, in Section 4, we observe that indoor white spaces exhibit interesting location correlation and channel correlation. These characteristics provide insights in identifying and utilizing indoor white spaces.

In Section 5, we present our indoor white space identification system, called WISER, which identifies additional indoor white spaces. To the best of our knowledge, this is the first system that can use the additional white spaces without requiring client devices to sense the spectrum. Our approach is rather general and can be additionally used in other spectrum monitoring applications. In Section 6, we present channel and location clustering algorithms to reduce the number of sensors used by WISER to track indoor white spaces.

In Section 7, we build a proof-of-concept WISER prototype, deploy it on one floor of a typical office building, and evaluate its performance by real-world experiments across a four-month duration. In particular, we demonstrate that WISER can identify 30%–40% more indoor white spaces with negligible false alarms, as compared to alternative baseline approaches.

Given that indoor environments are crowded and have the most spectrum demand, our system provides a new principled approach to make additional spectrum available in these environments. Last, we remark that WISER is not limited to the TV spectrum. It can be similarly applied to any other portion of the spectrum where DSA techniques will be adopted.

2 RELATED WORK

In FCC (2010), the FCC adopted the geo-location database approach for predicting (outdoor) white space availability at requested user locations. It has been widely used in academia, such as white

[2]For the purpose of identifying white spaces, an RF sensor consisting of USRP1, a TVRX receive-only daughter board and an antenna still costs around 1K U.S. dollars. Hence, reducing the total sensor cost is an important system design consideration.

space capacity analysis (Harrison et al. 2010; Makris et al. 2012; Hessar and Roy 2015) and networking (Feng et al. 2011; Murty et al. 2012; Chen and Huang 2013). However, there exist concerns about local accuracy of propagation models, since they do not properly account for built environments (e.g., man-made buildings), especially in dense urban areas. Indeed, the geo-location approach misses many vacant TV channels in a metropolis like Hong Kong (Yan and Chen 2011).

As a result, data-driven approaches based on local spectrum sensing are being explored due to improved local accuracy. Early measurement studies focused on temporal characteristics of long-term spectrum usage over a large frequency range at only a few selected outdoor locations in cities like Guangzhou (Yin et al. 2012), Singapore (Islam et al. 2008) Chicago (Taher et al. 2011), and so on. Recent efforts include dense spectrum measurements in small areas of several square meters (Phillips et al. 2012; Achtzehn et al. 2012; Palaios et al. 2014; Ying et al. 2015a) and large-scale drive tests covering areas up to hundreds of square meters (Achtzehn et al. 2014; Zhang et al. 2014) to capture spatial variations in spectrum usage. Collected outdoor spectrum data is often used to estimate signal strengths at unmeasured locations with statistical interpolation techniques (e.g., Kriging) as in Phillips et al. (2012) or improve propagation models as in Achtzehn et al. (2012) to augment geo-location databases. Following this line of research, Ying et al. (2015b, 2017) considered incentivized crowd-sensing for low-cost wide-area spectrum data collection, in which sensing tasks are outsourced to mobile users whose devices are equipped with spectrum sensors, and users who contribute data are compensated for resource consumption (e.g., battery and CPU) for sensing.

Compared to outdoor measurement campaigns, there exist much fewer indoor measurement studies, despite that 70% of spectrum demand comes from indoors (Chandrasekhar et al. 2008). Wellens et al. (2007) compared outdoor and indoor spectrum occupancy at two different locations in the band from 20MHz to 6GHz. Kliks et al. (2014) performed measurements at different indoor locations inside two buildings to study spatio-temporal stability of TV signals and quantify indoor attenuation by comparing them against rooftop measurements. König et al. (2014) collected indoor spectrum data in TV bands at an exhibition hall in Berlin (Germany) for six days with a network that consists of 21 spectrum sensors, and they analyzed duty cycles and spatial correlation of the measurements. Meshkova et al. (2013) set up an indoor testbed with 60 low-cost sensors covering a 20m-by-12m area, and they constructed indoor coverage maps from unreliable measurements using statistical interpolation. Fadda et al. (2015) conducted outdoor (i.e., on the roof) and indoor (i.e., on lower floors) measurements at 14 buildings of different characteristics, such as office/flat buildings and rural houses, in three cities in Europe. Authors further analyzed the results with respect to the hidden node margin problem, sensing parameters, and occupancy threshold. More recently, Liu *et al.* took indoor measurements at 66 locations on a single floor, and they applied Bayesian compressive sensing for identifying indoor white space (Liu et al. 2016).

In this work, we conduct a measurement campaign that collects both outdoor and indoor TV spectrum data at a much larger scale (up to 30+ diverse locations in Hong Kong at different time instants) than many prior studies. Furthermore, we focus on indoor white space and carry out comprehensive indoor measurement campaigns that consist of long-time sensing and one-time profiling (at up to 65 indoor locations) to study both temporal and spatial characteristics. Instead of using statistical interpolation techniques or indoor propagation models, we develop a novel data-driven system based on clustering techniques to identify indoor white space opportunities in a building.

3 INDOOR/OUTDOOR WHITE SPACE AVAILABILITY MEASUREMENT

3.1 Objective

We carry out a large-scale indoor/outdoor white space measurement in a typical metropolitan city, Hong Kong. The purpose of our measurement is twofold. First, we aim to understand the difference between the indoor and outdoor white space availability patterns. Such understanding motivates

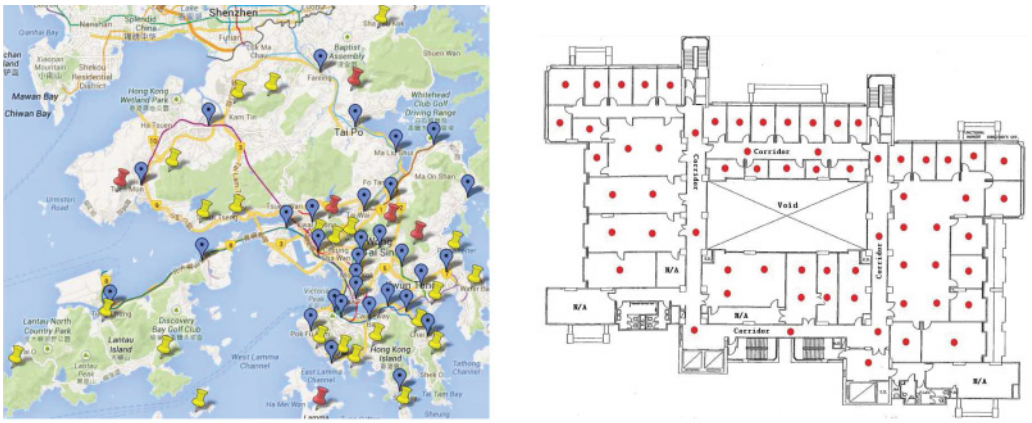

Fig. 1. (a) A map showing the 6 principal TV transmitting stations, 23 fill-in TV transmitting stations (CEDB 2016), and 31 diverse measurement locations that cover all 18 districts in Hong Kong. Principle and fill-in TV stations are labeled using red and yellow pin-shape markers, respectively. Measurement locations correspond to blue droplet-shape markers. Each measurement location is covered by 1–5 TV stations (2.2 on average) (OFCA 2016a), and the distance to its nearest TV station ranges from 0.97 to 9.35km (3.25km on average). (b) A map showing the 65 measurement locations (in red dots) on the seventh floor of a building. Each room has at least one measurement location at its center, and bigger rooms as well as corridors have multiple ones that are spread-out.

our investigation of indoor white space. Second, while various measurement studies have been reported in literature, we find a large-scale indoor/outdoor measurement campaign is missing for a metropolitan city. Such a large-scale measurement study is critical for properly evaluating the potential of white space networking in metropolises, where different districts exhibit diverse spectrum occupancy patterns.

3.2 Methodology

3.2.1 Equipment and Setup. Our measurement equipment consists of a USRP board (ETTUS 2016), a Log Periodic PCB Antenna, a laptop, and a battery bank. The USRP board is coupled with a TVRX receiver-only daughter board and a GNU Radio platform (Community 2016) to construct a spectrum analyzer, for measuring and detecting TV signals in the 470–806MHz spectrum band. Our device is calibrated against a RF signal generator to ensure accurate power reading in dBm. We use energy detection to detect analog signals by comparing the received power spanning 100KHz centered at their visual carriers against −104.2dBm. For digital TV signals, we use a feature-based detection scheme similar to that in Jallon (2008), which is able to detect digital TV signals as low as −96dBm/8MHz. More details can be found in our measurement report (Yan and Chen 2011).

3.2.2 Measurement Locations and Design. We measure indoor/outdoor white space availability at 31 different locations in Hong Kong, located in Hong Kong Island, Kowloon Peninsula, and New Territories. These locations cover all 18 districts of Hong Kong and have very different terrain and population characteristics (HKGov 2017). For example, the urban area such as MongKok has the world-highest population density, and skyscrapers have strong influence on signal propagation. While in remote areas like Yuen Lang, the population and tall-building densities are much lower. Figure 1(a) shows the 6 principal TV stations, 23 fill-in TV stations,[3] and 31 measurement locations.

[3]There are several tens of additional fill-in TV stations, but their precise location information is not available online, and we are unable to estimate their broadcasting coverage accordingly.

Table 1. Summary of the Indoor and Outdoor White Space Measurement Results

	Outdoor				Indoor				Indoor Bonus
	Urban	Sub-urban	Rural	Overall	Urban	Sub-urban	Rural	Overall	Overall
White Space Ratio (%)	44.1	55.9	60.9	53.6	67.9	74.7	73.3	72	18.4
Number of Vacant Channels	18.5	23.5	25.6	22.5	28.5	31.4	30.8	30.2	7.7
Total Vacant Spectrum (MHz)	148	188	204	180	228	251	246	242	62

More details (e.g., effective radiated power, polarization, etc.) about the TV broadcasting network of Hong Kong are available in OFCA (2016b). All measurement locations are in well-populated commercial/residential areas, and thus our measurement results capture the representative spectrum occupancy patterns in Hong Kong.

At each location, we measure indoor/outdoor spectrum occupancy of TV bands at three distinct time instants: morning, noon, and evening. Indoor measurements are taken inside various commercial buildings at selected locations. The time interval between two adjacent measurements is 4h. In each measurement, we scan all 42 analog/digital TV channels of 8MHz in the frequency range of 470–806MHz multiple times (OFCA 2012). For ease of discussions, they are labeled from CH 1 through CH 42. The feature-based detection scheme is used to identify locally unoccupied channels (i.e., white space) at each location.

3.3 Observations

Indoor and outdoor white space measurement results are provided in Table 1. Note that locations are categorized into urban, sub-urban, and rural areas, based on population density (HKGov 2017), and results are summarized for each area.

First, we observe that similar to the U.S. and Europe, there are a large number of vacant TV channels in Hong Kong—more than 50% of TV channels are white spaces. Together with prior measurement studies (McHenry et al. 2006; Islam et al. 2008; Yin et al. 2012), our results confirm abundant white space networking potential in metropolises. Second, rural areas have the most number of vacant channels, followed by sub-urban and urban areas. For example, in outdoor scenarios, rural and sub-urban areas have 7 and 5 more vacant channels than urban areas. Third, there are more vacant channels indoors than outdoors, mainly due to significant signal attenuation because of the blocking effects of walls. In particular, in indoor scenarios, an average of 72% of TV channels are white spaces, which is 18.4% higher than the outdoor scenarios. This corresponds to 7.7 additional vacant channels and 62MHz additional spectrum. Note that the amount of overall indoor white spaces is 242MHz, enough to support one additional Wi-Fi service in operation.

Furthermore, indoor white spaces are less fragmented than outdoor white spaces. The average length of contiguous vacant channels is 3.84 in indoor scenarios as compared to 1.87 in outdoor scenarios. This indicates that indoor white space is of better "quality," since it is easier for wireless devices to communicate over contiguous channels than over fragmented ones.

4 INDOOR WHITE SPACE CHARACTERISTICS MEASUREMENT

Complementary to our large-scale indoor/outdoor availability measurements, we also conduct intensive indoor measurements to gain necessary insight of indoor white space characteristics.

4.1 Methodology

4.1.1 Equipment and Setup. The same equipment described in Section 3.2.1 is used for this indoor measurement campaign, except that an omnidirectional antenna with a gain of 0dBi is used.

4.1.2 White Space Threshold. A TV channel is locally unoccupied if its received signal strength is less than or equal to a preset white space threshold, and occupied otherwise. Compared to feature-based detection, energy detection is faster but less sensitive. We adopt it to speed up the profiling process, which involves a large number of dense locations in an operational building. We set the white space thresholds to be −84.5dBm/8MHz for digital TV signals and −104.2dBm/100KHz for analog TV signals (centered at their visual carriers), respectively. These values are the maximum readings out of measured power spanning the corresponding bands in all empty channels based on long-time sensing results. While our thresholds for determining channel vacancy may seem aggressive due to hardware limitations, we believe that our observations are general and our system is not tied with these thresholds. We note that if improved hardware is in use to allow a highly conservative sensing threshold of −114dBm as suggested by the FCC, then the identified unoccupied channels are safe to use, in the sense that secondary users using these channels will not cause interference with primary TV users within a considerably large neighborhood. See FCC (2010) for detailed discussions on setting interference-safe sensing threshold for TV white space networking.

4.1.3 Measurement Locations and Design. As shown in Figure 1(b), a total of 65 indoor locations on one floor of a typical office building are selected for measurement. At each location, every channel is scanned five times. We observe <1% difference in recorded signal strengths beyond five time measurements. During each scanning, each channel is measured for 0.2s. The recorded signal is then processed by a GNURadio FFT program with a bin size of 2,048 and a resolution of 3.9KHz. We then record the maximum values observed at each bin for the channel during each scanning and compute the average value for that bin. For digital channels, we compare the received power over 8MHz centered at the middle of the channel against −84.5dBm. For analog channels, we compare the power spanning 100KHz centered at its visual carrier against −104.2dBm.

We conduct two types of indoor measurements: *indoor long-time sensing* and *indoor one-time profiling*. Indoor long-time sensing is for understanding temporal features of indoor white spaces. We measure received signal strengths for all TV channels at a typical indoor location consecutively for 96h. Indoor one-time profiling is to probe spatial features of indoor white spaces for a typical indoor environment. We mount the measurement equipment onto a movable cart and run a Python script to scan all TV channels automatically. We then profile indoor locations one by one. Profiling each location takes around 1.5min, and the whole process takes roughly 3h. We obtain a 65×42 matrix containing absolute signal strengths (in dBm) for 42 channels at 65 indoor locations. To facilitate comparison, we convert the absolute signal strengths to the relative signal strengths by comparing them against the corresponding white space thresholds. We collect a total of 13 one-time profiles in two periods in four months.

4.2 Long-Time Indoor Sensing Results

There are several observations from the long-time indoor sensing. First, from Figure 2(a), there are *strong* channels whose relative signal strengths exceed a large threshold most of the time. For

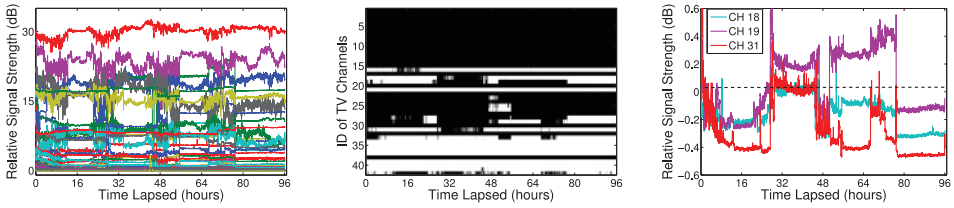

(a) (b) (c)

Fig. 2. (a) Relative signal strength (in dB) for all 42 TV channels in a 96h window. (b) Channel occupancy statuses for all 42 channels in the same 96h window. White spaces are denoted in white and occupied channels in black. (c) Three TV channels (CH 18, 19, and 30) that move up and down around the white space threshold (the dotted line). They are white spaces from time to time.

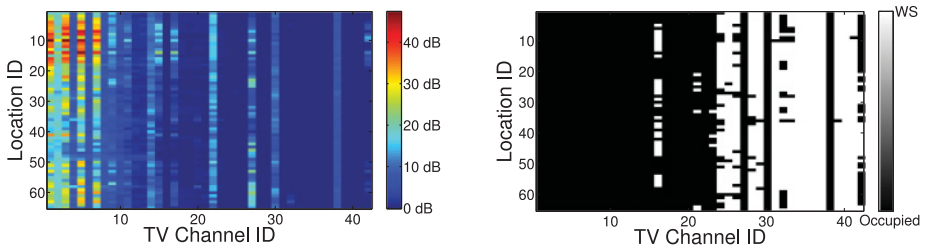

(a) (b)

Fig. 3. (a) Typical spatial map of channel relative signal strengths extracted from one-time spectrum profiling data. We observe signal attenuation patterns across different locations. (b) Typical spatial map of indoor white spaces (denoted in white, occupied channels in black) extracted from one-time spectrum profiling data. We observe different channel vacancy patterns across different locations.

instance, we observe 14.29% of channels with >10dB relative signal strength 95% of the time across the 96h interval, which means they are *long-term occupied* at the typical indoor location. Second, *weak-to-normal* channels follow a *short-term stable yet long-term unstable* pattern. Third, we observe intermittent white spaces availability from Figure 2(b). This is due to temporal signal strength variation in weak-to-normal channels. These observations suggest that to extract the maximum indoor white space potential, it suffices to identify strong channels via long-time sensing and then invest resources in tracking the slow-varying white space availability of weak-to-normal channels.

4.3 One-Time Spectrum Profiling Results

We have the following observations from one-time spectrum profiling results. First, as shown in Figure 3, there exists *spatial variation* in relative signal strength and white space availability for a channel at different indoor locations. It is mainly caused by complex outdoor and indoor signal propagation and attenuation patterns (e.g., due to blocking effects of indoor walls). This implies potential white space loss if indoor white space availability is directly inferred from outdoor availability results.

Second, seen from Figure 4(a), for a given channel, there is also strong correlation in signal strengths and white space availability across different locations. This suggests that we can infer channel vacancies at multiple correlated locations from one or a few representative locations. We refer to this observation as indoor white space *location correlation*.

In addition, seen from Figure 4(b), we observe that for multiple channels, there are strong correlations in their signal strengths and white space availability patterns across all locations. The

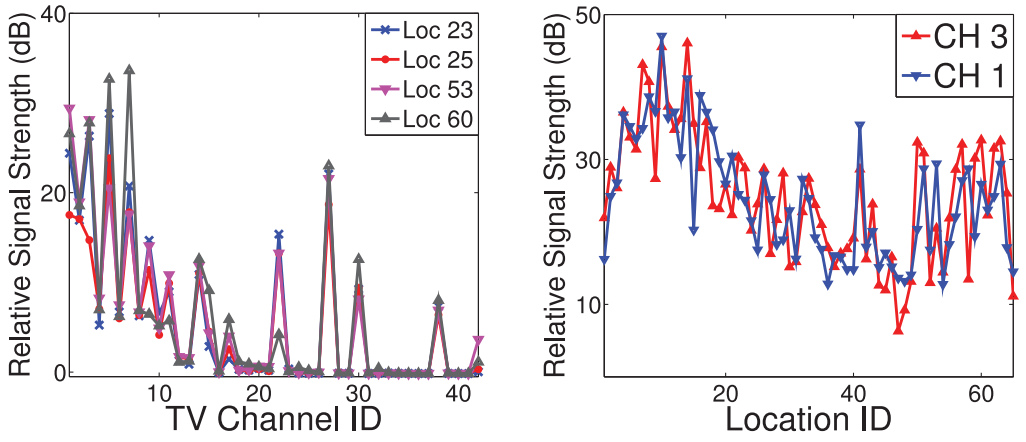

(a) (b)

Fig. 4. (a) Locations 23, 25, 53, and 60 receive similar signal strengths from many TV channels. Each line represents the relative signal strengths received at an indoor location for the 42 channels. We observe strong location correlation. (b) CH 1 and 3 exhibit very similar signal strengths at different indoor locations. Each line represents the relative signal strengths for a channel at 65 indoor locations. We also observe strong channel correlation.

similarities among these channels can be due to that they share the same transmission tower, similar loss and attenuation patterns in their propagation. This suggests that we can group these "similar" channels together into a group, and infer the vacancies of this group of channels from those of a representative channel in this group. We refer this observation as indoor white space *channel correlation*.

The above observations on location correlation and channel correlation are drawn from one-time profiling results. They have the potential to form useful guidelines in designing indoor white space identification systems. One important question that stands in the way, however, is *whether the correlation among channels and locations are stable across different time epochs*.

4.4 Stability of Indoor Channel Correlation and Location Correlation

To study the stability of channel correlation and location correlation, we cluster channels and locations according to their similarity using one-time profiling data collected across seven days in the first two-week period. We then compare one of the clustering results (e.g., the first day) with other clustering results. If channel and location correlations are stable over time, then we should see consistent clustering results in these seven days, and observe discrepancy in the results otherwise.

To filter out noise in profiling data while maintaining necessary information in signal strengths, we quantize relative signal strengths as described in Section 5.5.3. We then apply the clustering algorithms described in Section 6 and compute the Rand Index (Rand. 1971) of clustering results to examine their consistency. The Rand Index is commonly accepted as an objective criterion for comparing two clustering results. A Rand Index of 1 indicates two identical clustering results, and 0 indicates total disagreement.

To facilitate the illustration for Figure 5, we define *a channel group* as a group of channels that exhibit similar signal strengths across different indoor locations, and *a location group* as a group of locations that receive similar signal strengths for a particular set of channels. As shown in Figure 5(a), when we have three or more channel groups, the average Rand Index reaches 0.79 and

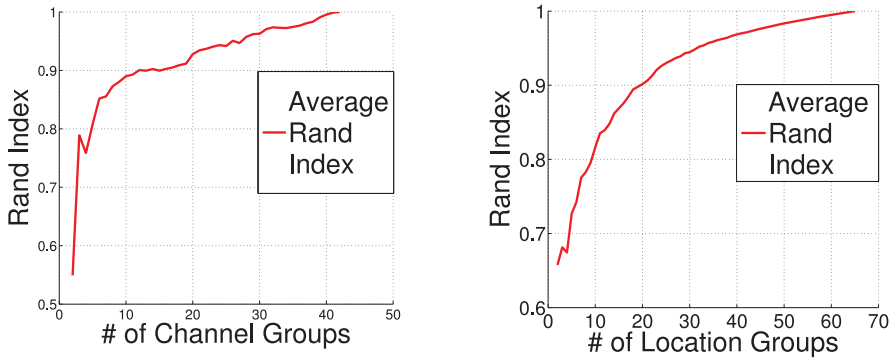

Fig. 5. (a) Channel correlation is consistent across different days. The input is a matrix of quantized relative signal strengths for 42 channels at 65 locations. We would obtain similar channel clustering results with more than three channel groups. (b) Location correlation is consistent across different days. The input is a matrix of quantized relative signal strengths at 65 locations for 4 channels (i.e., Ch 1, 3, 5, and 7). We would obtain similar location clustering results with more than five location clusters. In both figures, clustering result of data in the first day serves as a main reference. Both curves start with two groups. The Rand Index is 1 when there is only one group.

keeps rising. It means that we would obtain similar channel clustering results, and the channel correlation is consistent across different days. Figure 5(b) shows that the average Rand Index has exceeded 0.80 when there are 10 or more location groups for a group of channels (i.e., CH 1, 3, 5, and 7), which indicates that location correlation also exhibits consistency in time. These observations imply that *the correlations among channels and locations are very likely to be stable over time.* This insight is critical in gauging our designs of the indoor white space identification system.

4.5 Summary

In summary, our results from long-term sensing, one-time profiling, and correlation stability verification reveal the following useful observations:

(1) Strong channels are long-term stable; weak-to-normal channels are short-term stable but long-term unstable.
(2) *Location correlation*: given a channel, there are strong correlations in its signal strength and white space availability across multiple indoor locations; these correlations are stable in time.
(3) *Channel correlation*: there are strong correlations in multiple channels in their signal strengths and white space availability patterns across all locations; these correlations are stable in time.

The first observation suggests that to extract the maximum indoor white space potential, it suffices to identify strong channels via long-time spectrum sensing and track slow-varying white space availability of weak-to-normal channels. The remaining two observations suggest that we can focus on monitoring representative channels at representative indoor locations and inferring the availability of other channels at other locations by exploiting the location and channel correlations. These observations will be utilized in designing indoor white space identification systems in the next section.

5 WISER—WHITE SPACE INDOOR SPECTRUM ENHANCER

In this section, we first explore the design space of an indoor white space identification system. We then present the architecture of WISER, which consists of real-time sensing module, white space database, and indoor positioning module.

5.1 Design Objective and Design Space

A well-performed indoor white space identification system needs to (i) minimize false alarms (*safety*), and (ii) identify as many white spaces correctly as possible (*efficiency*). In addition, the sensor cost is also a major consideration, as RF sensors can be expensive. We define the following three metrics to evaluate a system:

(1) *False Alarm Rate (FA Rate):* the ratio between the number of channels that a system mis-identifies as vacant and the total number of vacant channels that the system identifies. A system with lower *FA Rate* is safer.
(2) *White Space Loss Rate (WS Loss Rate):* the ratio between the number of channels that a system mis-identifies as occupied and the total number of actually-vacant channels. A system with lower *WS Loss Rate* is more efficient.
(3) *Sensor Cost:* the total cost of all RF sensors in use.

Generally, there are several approaches to identify indoor white spaces. The *outdoor-sensing-only (OS-Only)* approach performs spectrum sensing locally on the rooftop using one outdoor sensor and only reports channels that are available outdoors for indoor use. Despite the low sensor cost, this approach is too conservative to be efficient, as it fails to take into account the significant attenuation on TV signals due to the blocking effects of indoor obstacles (e.g., walls).

Under the second approach called *one-time-profiling-only (OTP-Only)*, we only profile indoor locations once, then label every channel at each location as either 1 (vacant) or 0 (occupied), and store such information in the white space database for later retrieval. However, this approach assumes the indoor white space availability to be time-invariant, which does not hold according to our indoor white space measurements in Section 4. As a result, this approach fails in both safety and efficiency; in particular, violating safety may lead to serious interference to primary users.

The third approach is *sensor-all-over-the-place.* This approach deploys dense indoor sensors to monitor indoor white spaces. Although this scheme can achieve the ideal safety and efficiency, it comes with a significant deployment cost.

Making a compromise between the cost and the efficiency, the fourth approach is *sensor-over-random-place (Random-Sensor).* This approach deploys indoor sensors at part of the locations, so the indoor white spaces at the place with sensors could be utilized while maintaining an affordable cost. However, this approach cannot achieve an optimized performance.

In summary, none of the above approaches could achieve satisfactory performance at low cost. To tackle this problem, we develop an indoor white space identification system called WISER with optimized safety and efficiency at lower sensor cost as compared to the above baseline solutions.

5.2 WISER Overview

As shown in Figure 6, WISER consists of three components, namely, real-time sensing module, white space database, and indoor positioning module. WISER takes user locations as inputs and outputs indoor white space availability at requested locations.

5.3 Indoor Positioning Module

In WISER, a user determines its indoor location by using the indoor positioning module. Indoor positioning has been widely explored in recent years. Many wireless technologies can be integrated

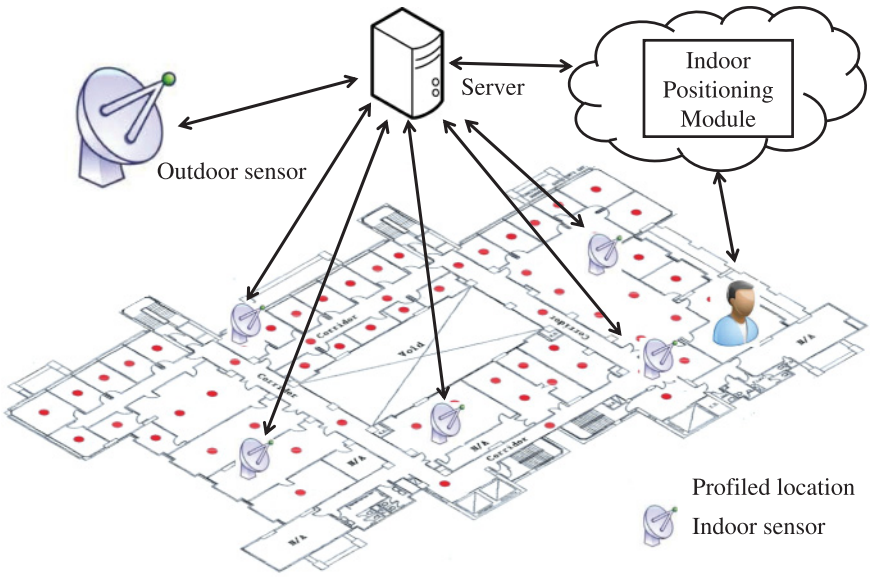

Fig. 6. Architecture schema of WISER.

into indoor positioning, including IR, ultrasound, RFID, WLAN, and Bluetooth. See Gu et al. (2009) for a recent survey. Since indoor positioning is developing into a mature technology, WISER simply uses one existing system as the indoor positioning module. It is conceivable that the indoor positioning accuracy will affect WISER's performance. We will study the relationship between indoor positioning accuracy and the performance of WISER in Section 7.

5.4 White Space Database

The white space database receives real-time channel signal strengths reported from the sensors in the real-time sensing module, based on which white space availability is updated in real-time. After obtaining its indoor position, a user queries the white space database to retrieve a list of vacant channels for communication using a separate white space networking infrastructure. To handle dynamics of wireless microphones, wireless microphone users are suggested to register the location and frequency usage to the white space database, so WISER can exclude the frequency occupied by wireless microphone at the location and within its estimated interfering neighborhood from the returned list.

5.5 Real-Time Sensing Module

Given an indoor environment, the real-time sensing module performs real-time outdoor and indoor spectrum sensing and reports the results to the white space database. To realize this functionality, we first conduct one-time spectrum profiling at a sufficient number of indoor locations. To exploit the observation in long-time measurement (Section 4.2), we then group the channels into strong and weak-to-normal channels. We also identify some permanently available channels based on the long-time outdoor sensing and focus on the remaining weak-to-normal channels. Then, we perform channel-location clustering to leverage channel and location correlations (Section 4.3). Last, we place indoor sensors based on the results of channel-location clustering to optimize the use of a limited number of sensors and let them send real-time data to the server periodically.

5.5.1 One-Time Spectrum Profiling. One-time spectrum profiling aims to learn the indoor white space characteristics, including channel and location correlations. These locations should be as dense as possible. For example, in our study, 65 measurement locations are profiled including almost every room and corridor on an indoor floor, as shown in Section 4.4. For a non-profiled location, its indoor white space availability is assumed to be the same with the nearest profiled one. The profiling data will serve as the main reference to determine indoor sensor locations. Ideally, we should profile all measurement locations simultaneously. However, since we observed that indoor white spaces tend to be stable with moderate variation in the short term (e.g., hours), we base WISER deployment on the asynchronous one-time profiling within 3h.

5.5.2 Channel Grouping. We first group TV channels into two basic classes: strong channels and weak-to-normal channels (including permanently vacant channels), based on one-time and long-time measurements. Weak-to-normal channels have a higher chance to be white spaces due to signal variation and attenuation.

We motivate the simple grouping scheme with the following reasons. First, such classification is general. In fact, for a particular area, TV services are broadcast via one or more major TV towers in several channels. These channels usually carry strong signals and are distinguishable from others. In addition, due to stable TV broadcasting arrangement in the long run (e.g., years), the obtained grouping result will also be stable accordingly unless dramatic changes occur (e.g., shutdown of a TV tower). Moreover, it is efficient to group channels into two such basic classes. Because, by exploiting the "always on" nature of some TV channels, indoor sensors can focus on other time-varying channels rather than these stably strong ones.

5.5.3 Channel-Location Clustering. Channel-location clustering produces *channel-location (CL) groups*, each containing locations with similar signal strengths for channels with similar propagation patterns. In our current solution, we obtain CL groups by first clustering the channels according to their received signal strengths across the locations. Then, for each channel cluster, we group the locations according to the received signal strength distribution among those channels. More details will be described in Section 6. Nonetheless, conducting joint channel-location clustering is an alternative method and is left for future work.

To reduce the undesirable impact of noise, we introduce a *uniform quantizer* for received signal strengths before conducting channel-location clustering, which is defined as

$$S_q = \begin{cases} -1, & S_r \leq 0 \\ \left\lfloor \frac{S_r}{Q} \right\rfloor, & S_r > 0 \end{cases}, \tag{1}$$

where S_r is the received relative signal strength compared to the pre-set white space thresholds, Q is the quantization step (e.g., 5 dB), and S_q is the quantized relative signal strength.

5.5.4 Indoor Sensor Placement. Given a set of CL groups, we aim to deploy indoor sensors to fulfill (i) *coverage* requirement: every CL group is covered by at least one sensor, and (ii) *performance* requirement: safety is guaranteed and efficiency is maximized, given a number of indoor sensors. The brute-force way is to enumerate all possible configurations to find the best one. Instead of adopting this inefficient approach, we propose a greedy algorithm that could achieve local optimum with guaranteed system performance, as described in Section 5.

To avoid interference with primary users, indoor white space availability shared within each CL group is derived from real-time sensing results in a conservative way. First, if a particular CL group is covered by multiple indoor sensors, indoor white spaces are determined by comparing

the maximum received signal strength for a channel with the white space thresholds as follows:

$$WS(C_x) = \begin{cases} 1, & S_{max}(C_x, L_{sensors}) < WSThr_x \\ 0, & otherwise \end{cases}, \tag{2}$$

where $WS(C_x)$ means the white space availability for channel x at all locations in the CL group, $S_{max}(C_x, L_{sensors})$ means the maximum received signal strength among multiple sensor locations for channel x in the CL group, and $WSThr_x$ is the white space threshold for channel x.

Second, if a CL group is covered by only one indoor sensor, a *protection range* (in dBm) needs to be added to minimize false alarm rate as follows:

$$WS(C_x) = \begin{cases} 1, & S(C_x, L_{sensors}) < WSThr_x^* \\ 0, & otherwise \end{cases}, \tag{3}$$

where $WSThr_x^* = WSThr_x - PR_x$, and the PR_x is the protection range for channel x for this CL group. To exploit the statistics of received channel signal strength deviation in a CL group in training data sets, we obtain PR_x by multiplying a constant (6 by default) with the standard deviation of all received signal strengths in channel x at locations in the CL group. This constant measures how conservative we are. It can be used to control the FA rate.

6 ALGORITHM

In this section, we first discuss the intuition of our algorithms for the real-time sensing module. We then present the channel-location clustering and indoor sensor placement algorithms. At the end, we provide complexity analysis of proposed algorithms.

6.1 Algorithm Intuition

As revealed in Section 4.4, there exists consistent correlation among channel signal strength at different locations. An intuitive way to extract such correlation is clustering. We first perform channel clustering, then, we carry out location clustering for each channel group.

In this way, we obtain CL groups (recall that CL group stands for channel-location group). Within each CL group, the channels share similar signal strength at the locations; hence, intuitively, we can use one sensor per CL group to monitor signal strengths of the channels (in the group) at the locations (in the group). Following the above intuition, we design Algorithms 1 and 2 with agglomerative clustering method (Xu and Wunsch 2005) and Algorithms 3 and 4 with Fuzzy C-Means clustering method (Bezdek 1981). As the next step of the above intuition, we need to deploy one sensor (or more) per CL group (i.e., coverage requirement), and enable WISER to correctly identify as many indoor white spaces as possible (i.e., performance requirement). These two requirements are very important in designing our indoor sensor placement algorithm (Algorithm 5) and its ranking mechanism (Algorithm 6). More details will be discussed later in this section.

6.2 Proposed Algorithm

The proposed algorithm takes quantized relative signal strengths and the number of indoor sensors as inputs and then outputs a list of sensor locations. In the case of multiple feasible sensor placement options, the one with least FA rate (with first priority) and least WS Loss rate is chosen, namely, "least-false-alarm-first" criterion.

6.2.1 Channel-Location Clustering. As stated in Section 5.5.3, the channel-location clustering aims to cluster locations that receive similar channel signal strength for certain channels into the same group. We do so by first grouping the channels according to their signal strengths at all indoor locations and then within each channel group clustering the locations.

As mentioned in Section 6.1, we need to deploy a given number of sensors for CL groups. One straightforward way to determine the number of CL groups is to let it be equal to the number of sensors. With a larger number of CL groups, we may not guarantee the coverage requirement; with fewer CL groups, it tends to be a waste of sensor resources, which is undesirable. Provided a number of CL groups, the next question is how to decide the desirable number of channel clusters and also the desirable number of location clusters for each channel group. There are various ways to probe the true number of clusters, including a model-based approach (Fraley and Raftery 1998). In this study, we are more interested in the relationship between the number of indoor sensors and system performance instead of seeking for the true number of channel or location clusters. We will leave the discussion of the relationship between the number of indoor sensors and system performance to the next section.

ALGORITHM 1: Channel Clustering via AC

Input: S: the $M \times N$ training data set {M is the total number of locations, N is total number of channels to be clustered};
k: the number of channel clusters
Output: k channel clusters with sizes of $M \times n_1, M \times n_2, \ldots, M \times n_k$, where $\sum_{i=1}^{k} n_i = N$

```
if k == N then
    return N channel clusters of size M × 1
let each channel object (M × 1) be a cluster
compute the proximity matrix
do
    merge two "closest" clusters based on the linkage criterion
    update the proximity matrix
while more than k clusters remain;
return k channel clusters with sizes of M × n_1, M × n_2, ..., M × n_k, where Σ_{i=1}^{k} n_i = N
```

ALGORITHM 2: Location Clustering via AC

Input: S_i: the $M \times n_i$ channel cluster {M is the total number of locations to be clustered, n_i is total number of channels};
k_i: the number of location clusters
Output: k_i location clusters with sizes of $m_1 \times n_i, m_2 \times n_i, \ldots, m_{k_i} \times n_i$, where $\sum_{j=1}^{k_i} m_j = M$

```
if k_i == M then
    return M location clusters of size 1 × n_i
let each location object (1 × n_i) be a cluster
compute the proximity matrix
do
    merge two "closest" clusters based on the linkage criterion
    update the proximity matrix
while k_i clusters remain;
return k_i location clusters with sizes of m_1 × n_i, m_2 × n_i, ..., m_{k_i} × n_i, where Σ_{j=1}^{k_i} m_j = M
```

As mentioned in Section 6.1, we consider two representative clustering algorithms in this work: agglomerative clustering and Fuzzy C-Means clustering.

6.2.2 Agglomerative Clustering (AC). In Agglomerative clustering, each data point starts as a cluster, and clusters are merged iteratively until the desirable number of clusters is obtained. In our algorithm design, we adopt Ward's minimum variance method (Jr 1963) as the linkage criterion, and Euclidean distance as the similarity metric due to their widespread popularity.

Given one-time profiling data, we treat signal strengths across different indoor locations for a channel as a feature vector and cluster similar channels together to obtain channel clusters. Then, we treat signal strengths in different channels of the channel group at a location as a feature vector and perform location clustering accordingly.

For the number of clusters, in our current solution, we enumerate all possible numbers of channel clusters and assign numbers of location clusters to channel clusters that are proportional to sizes of channel clusters. For instance, given 20 CL groups, we may try out 3 (or other possible numbers from 1 to 20) channel clusters and obtain clusters with sizes of 8, 16, and 16 via channel clustering. Then, we will assign 4, 8, and 8 location clusters to 3 channel clusters, accordingly,

before location clustering. Note that when multiple combinations are possible, WISER will choose the one according to the "least-false-alarm-first" criterion.

The channel clustering algorithm is illustrated in Algorithm 1. As shown in Lines 3 and 4, we let each channel object be a cluster at the initial stage and compute the pair-wise proximity matrix (i.e., Euclidean distance). Then, we apply Ward's minimum variance method to merge the two "closest" clusters and update the proximity matrix accordingly (Lines 6 and 7). We repeat the process until a required number of clusters is obtained. In the case of multiple training data sets as the input, we can extend the dimension of channel objects by treating signal strengths across different locations across different days for a channel as a two-dimension vector, and we perform channel clustering in the same way. One potential advantage of training with multiple data sets is that we can improve clustering accuracy and robustness against the noise in individual data sets. The location clustering algorithm (Algorithm 2) is conducted in a similar way, except that we let the vector containing signal strengths in different channels at a location be a location object during the whole process.

ALGORITHM 3: Channel Clustering via FCM

Input: S: the $M \times N$ data set {M is the total number of locations, N is total number of channels to be clustered}
c: the number of channel clusters

Output: U: the membership coefficient matrix, $U = [u_{i,j}]_{c \times N}$ {Membership coefficient of the jth channel in the ith cluster};
V: the $M \times c$ matrix for the means of the c clusters;
E: cluster for each channel

1 **do**
2 Update $U : u_{ij}^{(t+1)} = \frac{1}{(\sum_{l=1}^{c}(D_{lj}/D_{ij})^{1/(1-m)})}$;
3 Update $V : v_i^{(t+1)} = \frac{(\sum_{j=1}^{N}(u_{ij}^{(t+1)})^m x_j)}{(\sum_{j=1}^{N}(u_{ij}^{(t+1)})^m)}$;
4 **while** $||V^{(t+1)} - V^{(t)}|| \geq \varepsilon$;
5 $e_j \leftarrow$ the cluster i with $u_{ij} > 1/c$;
6 **return** *U, V, E*

ALGORITHM 4: Location Clustering via FCM

Input: S: the M mean vector of channel clusters {M is the total number of locations to be clustered}
c: the number of location clusters

Output: U: the membership coefficient matrix, $U = [u_{i,j}]_{c \times M}$ {Membership coefficient of the jth location in the ith cluster};
V: the c mean vector of the c clusters;
E: cluster for each location

1 **do**
2 Update $U : u_{ij}^{(t+1)} = \frac{1}{(\sum_{l=1}^{c}(D_{lj}/D_{ij})^{1/(1-m)})}$;
3 Update $V : v_i^{(t+1)} = \frac{(\sum_{j=1}^{M}(u_{ij}^{(t+1)})^m x_j)}{(\sum_{j=1}^{M}(u_{ij}^{(t+1)})^m)}$;
4 **while** $||V^{(t+1)} - V^{(t)}|| \geq \varepsilon$;
5 $e_j \leftarrow$ the clusters i with the first two maximum value of u_{ij};
6 **return** *U, V, E*

6.2.3 Fuzzy C-Means Clustering (FCM). Fuzzy C-Means is another widely used clustering algorithm that can obtain a fuzzy decision boundary between different clusters. Instead of clustering a boundary location into only one of the multiple possible clusters, it allows us to associate every location with a set of probabilities, each representing the "likelihoods" of it belonging to a possible cluster. This way, we can combine white-space availability information of this boundary location from multiple possible clusters to obtain accurate results. The design of this algorithm is similar to that of agglomerative clustering, except the following parts:

(1) The outputs of channel location clustering are different. After clustering, for agglomerative clustering, a location can only belong to one CL group. For Fuzzy C-Means clustering algorithm, a location can "belong" to multiple CL groups. Specifically, for each location, the algorithm will output a set of "likelihoods" of this location belonging to possible clusters.
(2) The inputs for location clustering are different. For agglomerative clustering, we let the vector containing signal strengths in different channels at a location be a location object,

and it is the input for location clustering. For Fuzzy C-Means clustering algorithm, for each channel group, we set the "means" vector obtained from channel clustering as the input. The "means" vector of a channel group is the vector of signal strengths of the "center" channel (of this channel group) across all the 65 locations.

(3) The ways of setting protection ranges are different. During white space identification, for agglomerative clustering algorithm, we set the protection range to be 6 times of the standard deviation of all received signal strength in channel x at locations in the CL group. For Fuzzy C-Means clustering algorithm, we set the protection range to be 6 times of the standard deviation of all received signal strength in channel x at locations in the CL group when the number of sensors is so small that each location can only belong to one location group. Otherwise, we set the protection range for this group to be one standard deviation of all received signal strength in channel x at locations in the CL group.

The channel clustering algorithm is illustrated in Algorithm 3. At first, the "Mean Vector" V is initialized randomly. D_{ij} stands for the distance between channel i and "mean" v_j, the fuzzy parameter m is usually set to be 2. As shown in Lines 2 and 3, we continuously update U and V until V converges. The output will not only contain the cluster of the channels, but also the "means" of each cluster. The location clustering is conducted in a similar way (Algorithm 4), except that we let the output "Means Vector" from the channel clustering be the input and cluster them in the location dimension.

As we will show in Section 7, both clustering algorithms achieve decent performance.

ALGORITHM 5: Indoor Sensor Placement

Input: s: given sensor quota
Output: L: a set of sensor locations
1 **Initialization**: $L \leftarrow NULL$
2 **while** *uncovered Channel-Location group exist* **do**
3 $C \leftarrow$ remaining ranked candidate locations
4 **for** $i = 1$ *to length(C)* **do**
5 **if** $C[i]$ *can cover any not-covered Channel-Location group* **then**
6 $L \leftarrow L + C[i]$
7 $N \leftarrow N - 1$
8 **break**
9 **if** $length(L) < s$ **then**
10 $C \leftarrow$ ranked remaining candidate locations
11 $L \leftarrow$ first $(s - length(L))$ candidates in C
12 **return** L

ALGORITHM 6: Candidate Location Ranking

Input: S: already selected sensor locations, C: candidate locations
Output: C': ranked candidate locations
1 **Initialization**: $F \leftarrow NULL$ {FA rate}, $W \leftarrow NULL$ {WS Loss rate}
2 **for** $i = 1$ *to* $length(C)$ **do**
3 $S' \leftarrow S + C(i)$
4 $[f', w'] \leftarrow$ evaluated performance for S'
5 $F[i] \leftarrow f'$
6 $W[i] \leftarrow w'$
7 $C' \leftarrow$ ranked locations according to (F, W)
8 {Candidate locations with less FA rate (first priority) and less WS Loss rate get higher ranking}
9 **return** C'

6.2.4 Indoor Sensor Placement. As mentioned in Section 5.5.4, we need to meet coverage and performance requirements in determining sensor location based on channel-location clustering results. To avoid brute-force enumeration of indoor sensor locations (e.g., C_{65}^{s} given 65 indoor locations and s indoor sensors), we introduce a greedy sensor placement algorithm as shown in Algorithm 5. Initially, all CL groups are not covered, and all indoor locations are candidates for sensor placement. We rank candidates according to their ranks (Line 3). More details about the

ranking algorithm (Algorithm 6) will be illustrated later. In Lines 4–8, we check for each candidate one by one, starting from the highest ranking one, whether any not-covered CL groups can be covered if we place one sensor at that location. If yes, then we remove the covered CL groups from the not-covered list, add this location to the sensor location pool, and repeat the process for the remaining candidate locations; otherwise, we exam the next candidate until a suitable one is found. Our algorithm terminates the while loop (Line 2–8) when all initially not-covered CL groups are covered by at least one sensor. Since one indoor location may belong to different CL groups with respect to different channel groups, it is possible that we are able to cover multiple CL groups by deploying one sensor and cover all CL groups with fewer sensors. Hence, upon the termination of the while loop, our algorithm guarantees that all CL groups will be covered. If there are still additional quota for sensor locations, then we rank remaining candidates again and choose higher-ranking locations consecutively until the expected number of sensor locations is reached (Lines 9–11).

The ranking algorithm is crucial in fulfilling the performance requirement, as illustrated in Algorithm 6. At each stage, we rank candidate locations by comparing their "contribution" to the overall performance, which is quantized in items of evaluated FA rate and WS Loss rate after their individual participation in the current sensor pool. In Lines 3–6, we first add a candidate location to existing sensor location pool and then compute corresponding FA rate and WS Loss rate f' and w'. We repeat the process for all candidate locations and then compare their FA rates and WS Loss rates. By applying the "least-false-alarm-first" criterion, we will finally obtain the desirable ranking for given candidate locations (Line 7).

6.2.5 Complexity Analysis. In this section, we analyze the complexity of proposed algorithms. In Algorithm 1 (channel clustering via AC), since it takes $O(M)$ to compute the Euclidean distance between two channel objects (each is represented by a Mx1 vector), and there are a total number of $O(N^2)$ pairs of channel objects, the complexity of computing the proximity matrix is $O(MN^2)$. In the merging phase, each channel object is treated as a cluster. We can use a minimum heap of size $O(N)$ to store each cluster and its closest cluster as a node and their cluster distance as the key of the node. It takes $O(N \log N)$ time to construct such a heap and constant time to find and merge the two closest clusters at the top of the heap to a new cluster. Then, calculating the cluster distance between the new cluster and remaining clusters in the heap takes $O(N)$ time, and insertion takes $O(\log N)$. Since we will merge $(N - k)$ times, the overall complexity of merging is $O(N^2)$. Therefore, the complexity of Algorithm 1 is dominated by proximity matrix construction, which is $O(MN^2)$. Similarly, the complexity of Algorithm 2 (location clustering via AC) is $O(n_i M^2)$, for the ith channel cluster of size M-by-n_i.

In Algorithm 3 (channel clustering via FCM), each iteration takes $O(MNc^2)$ time for computation, where c is the number of clusters. Then, the overall complexity of Algorithm 3 is $O(iMNc^2)$, and so is Algorithm 4 (location clustering via FCM), where i is the number of iterations.

Then, we analyze the complexity of Algorithm 6 (candidate location ranking), since it is a subroutine of Algorithm 5 (indoor sensor placement). In Algorithm 6, it takes $O(MN)$ to compute FA and WS loss rates for a sensor placement scheme, because each channel (N in total) at each location (M in total) needs to be evaluated. Since the number of candidate locations is $O(M)$, the overall complexity of Algorithm 6 is $O(M^2N)$. For Algorithm 5, the while loop runs up to s iterations. In each iteration, Algorithm 6 is called to rank candidate locations, which is the most dominant operation. Therefore, the overall complexity of Algorithm 5 is $O(sM^2N)$.

7 PROOF-OF-CONCEPT WISER PROTOTYPE AND EXPERIMENTS

In this section, we deploy a proof-of-concept WISER prototype and conduct actual experiments across four months to evaluate its performance. The WISER prototype takes user's indoor position

as input and then outputs a list of vacant channels at the position. Our objectives are: (i) evaluating the performance of WISER prototype and comparing it with alternative solutions in a typical indoor scenario; (ii) demonstrating its ability of providing accurate indoor white space information across a long period of time (in this case four months), and there is no need to re-configure WISER frequently; (iii) demonstrating how to choose a suitable number of indoor sensors for the target indoor scenario; (iv) illustrating the impact of indoor positioning errors on WISER's performance.

7.1 Scenario and Settings

7.1.1 Scenario. We build a proof-of-concept WISER prototype for one floor of a typical office building to evaluate its performance using actual experiments. As shown in Figure 1(b), this scenario contains individual office rooms with various sizes, common rooms of larger sizes, and corridors, all of which are separated by walls or glass. We use the set of 13 indoor one-time profiles collected during the months between October 2012 and March 2013 using the methodology in Section 4.1.3. The experimental dataset is of size $13 \times 65 \times 42$, and each one-time profile corresponds to a 65×42 matrix, which represents the received signal strengths (in dBm) at 65 locations for 42 TV channels.

7.1.2 Settings. We set the white space threshold to be −84.5dBm/8MHz for digital TV channels and −104.2dBm/100KHz for analog channels. To capture real-world outdoor sensing, we perform outdoor long-time sensing for 30h by placing the equipment on the rooftop. We observe 5 channels of which signal strengths are always far below the white space threshold, and hence treat them as outdoor-sensor-reported white spaces. We also remove 11 long-term strong channels (whose received signal strengths are 10dB higher than the white space threshold) that have little chance to be white spaces indoors, even in the presence of signal attenuation, and we focus on tracking the availability of the remaining channels to maximally extract the indoor white space potential.

To ensure the quality of channel-location clustering, we use two sets of one-time profiling data as inputs into the clustering algorithm. We are aware of the potential over-fitting problem in clustering, and with only one one-time profiling data set, the deployed WISER tends to cause severe false alarms in the future prediction. It turns out that WISER can effectively alleviate the potential over-fitting problem by using two data sets. We use the remaining 11 data sets for actual experiments.

7.2 Performance Evaluation

For any indoor WS identification system, we are interested in the FA Rate and WS Loss Rate as defined in Section 5.1. The objectives of this experiment are (i) to quantify the performance of our WISER prototype using the above two metrics, (ii) to compare the performance of WISER against three alternatives: OS-Only, OTP-Only, and Random-Sensor, discussed in Section 5.1, and (iii) to demonstrate WISER's ability to provide accurate white space information in a long period of time.

In this experiment, the WISER prototype consists of a total of 20 indoor sensors and one outdoor sensor. OTP-Only labels channels at each location as 0 (occupied) or 1 (available), based on one of the training data sets for the WISER prototype, and uses this information to report white spaces in the future. Random-Sensor includes 20 indoor sensors and one outdoor sensor. The indoor sensors are placed at the 20 locations with the most white spaces in the training data set. This approach reports the white spaces obtained by the indoor sensors and the outdoor sensing result, while any channel at the locations without sensors are regarded as occupied unless the outdoor sensing result shows that the channel is free. We assume perfect indoor positioning accuracy at this stage and will study the impact of indoor positioning errors in Section 7.4.

We have several observations. First, as shown in Tables 2 and 3, our WISER prototype with different clustering algorithms are able to identify 30–40% more white spaces with negligible average

Table 2. Extra White Spaces and FA Rate Achieved by WISER Prototype with Agglomerative Clustering Algorithm as Compared to the OS-Only Approach in Eleven Experiments Across Four Months

Exp. ID	1	2	3	4	5	6	7	8	9	10	11	Avg.
Extra White Space (%)	28.81	33.53	30.67	34.20	31.76	34.02	34.96	29.59	34.43	34.90	35.02	32.90
WISER FA Rate (%)	0.16	0	0	0	0	0.25	1.16	0	0.16	0.44	0.42	0.24

Table 3. Extra White Spaces and FA Rate Achieved by WISER Prototype with Fuzzy C-Means Clustering Algorithm as Compared to the OS-Only Approach in Eleven Experiments Across Four Months

Exp. ID	1	2	3	4	5	6	7	8	9	10	11	Avg.
Extra White Space (%)	30.97	34.20	38.10	33.80	29.68	36.29	28.66	33.37	29.16	34.10	33.33	32.88
WISER FA Rate (%)	0	0	0.29	0	0	0.25	0	0	0.17	0	0.15	0.08

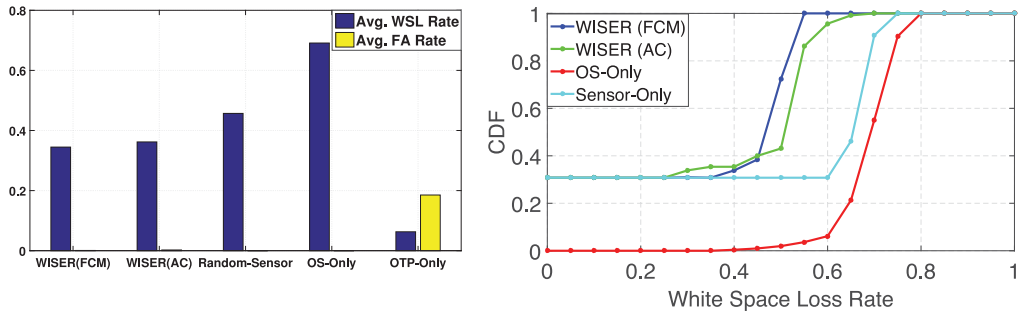

(a) (b)

Fig. 7. (a) Averaged FA rate and WS Loss rate for WISER(FCM), WISER(AC), Random-Sensor, OS-Only, and OTP-Only. The FA rate is 18.53% for OTP-Only, which may cause severe interference to primary users. As compared to OS-Only, WISER(AC) and WISER(FCM) are able to report 32% more white spaces on average with negligible FA rate. (b) CDF curves of average WS Loss rate for WISER(FCM), WISER(AC), Random-Sensor, and OS-Only. With OS-Only, 90% of the locations would suffer a WS Loss rate of 60%, even with Random-Sensor, 70% of the locations would suffer a WS Loss rate of 60%. This number is less than 5% for both WISER(AC) and WISER(FCM). Note that we excluded OTP-Only from this comparison, as OTP-Only will result in high FA rate despite its seeming high WS Loss rate, which makes it undesirable in the first place. Also, we did not plot the CDF curves for the FA rate for WISER(AC), WISER(FCM), OS-Only, and Random-Sensor, as all of them result in negligible FA rate, and their CDF curves for the FA rate are not informative.

FA rate (i.e., 0.24%, 0.08%), as compared to OS-Only. Specifically, Figure 7(a) shows a comparison among different approaches. As seen, OTP-Only is not suitable for identifying indoor white spaces in long term due to its unacceptable FA rate. WISER with Fuzzy C-Means clustering algorithm (denoted as WISER(FCM)) can achieve a better performance than WISER with agglomerative clustering algorithm (denoted as WISER(AC)), and they both outperform OS-Only and Random-Sensor. Second, WISER is able to provide accurate indoor white space information with negligible false alarms across a long period of time—four months in our experiments. Note that as WISER is built on channel-location correlations that are determined by surrounding environments, such as building structures, nearby buildings, and so on, it needs to be re-calibrated when environment changes

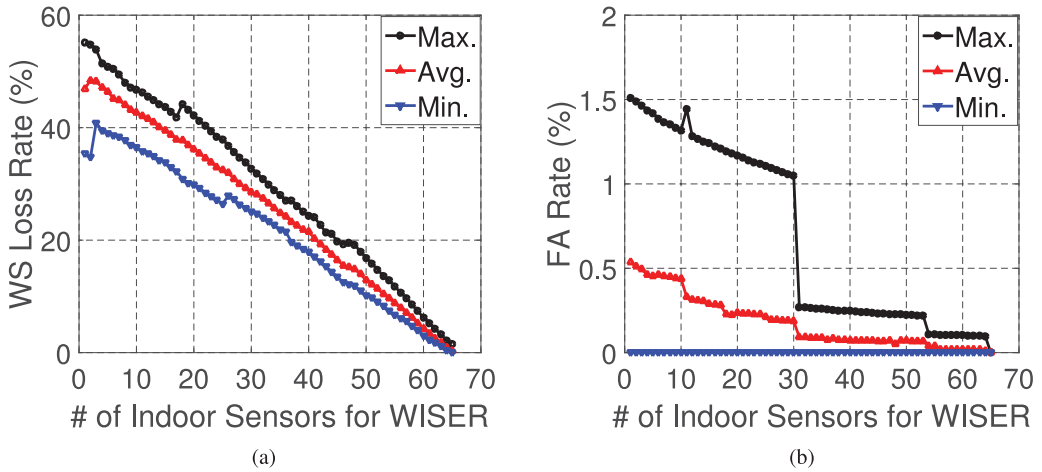

(a) (b)

Fig. 8. (a) The average, minimum (best-case), and maximum (worst-case) WS Loss rate vs. the number of indoor sensors. The more indoor sensors are used, the lower WS Loss rate WISER(AC) is able to achieve. (b) The average, minimum (best-case), and maximum (worst-case) FA rate vs. the number of indoor sensors. The FA rate tends to get lower when the number of indoor sensors increases. The average rate becomes stable when there are more than 11 indoor sensors.

substantially (e.g., a skyscraper is built nearby). Although WISER with agglomerative clustering algorithm may give a FA rate of 1% occasionally, one can systematically lower WISER's FA rate by using the other clustering algorithm—Fuzzy C-Means clustering algorithm, using more training data sets as inputs and using more conservative signal strength threshold in determining white spaces. We believe that our principled design behind WISER is general and does not depend on particular choices of system design parameters and inputs.

7.3 Number of Indoor Sensors to Use in WISER

For a specific indoor scenario, it is important to balance between WISER performance and the sensor cost. To understand their relationship, we vary the number of indoor sensors during WISER deployment and evaluate WISER performance in actual experiments under the same setting.

As shown in Figure 8, for WISER with agglomerative clustering algorithm, the WS Loss rate and FA rate decrease as more sensors are used. Note that the average FA rate drops to 0.4% when there are over 11 indoor sensors and remain rather low afterwards. To meet certain safety requirements (e.g., less than 0.4% average FA rate, as an example), the optimal number of indoor sensors would be 11; if the worst-case FA rate needs to be not much larger than 1.0%, WISER(AC) requires a minimum of 20 indoor sensors.

Figure 9 shows that, for WISER with Fuzzy C-Means clustering algorithm, the WS Loss rate and FA rate decrease as the number of sensors increase. Especially, the worst-case FA rate decreases dramatically and remains low afterwards. The average FA rate is always smaller than 0.4%. If the safety requirement is that the worst-case FA rate should be lower than 1%, then WISER (FCM) can achieve the requirement as long as the number of sensors is larger than 4.

In practice, we would jointly consider safety, efficiency, and sensor cost to determine the optimal number of indoor sensors. It also implies that for a typical indoor scenario, we could conduct multiple sets of one-time profiling, using some of them for WISER deployment and others for probing the suitable sensor number.

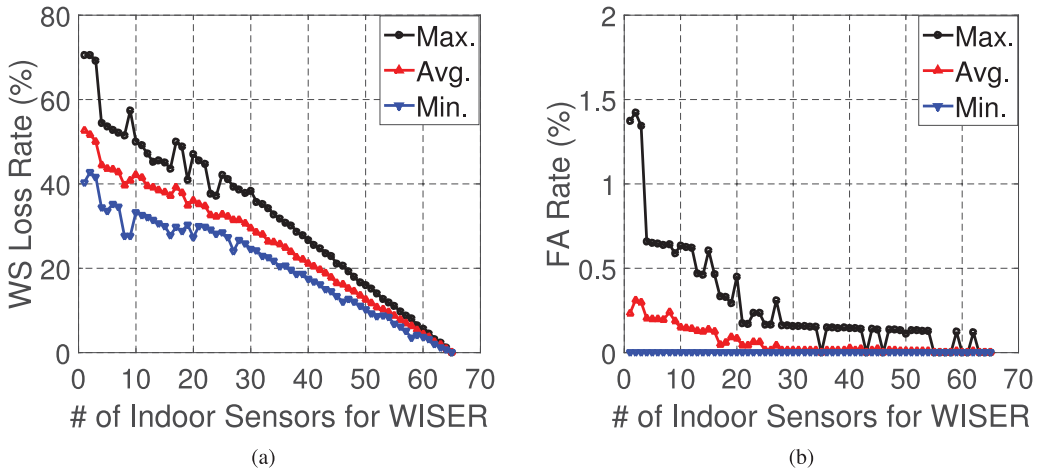

(a) (b)

Fig. 9. (a) The average, minimum (best-case), and maximum (worst-case) WS Loss rate vs. the number of indoor sensors. The more indoor sensors are used, the lower WS Loss rate WISER(FCM) is able to achieve. (b) The average, minimum (best-case), and maximum (worst-case) FA rate vs. the number of indoor sensors. The FA rate tends to decreases when the number of indoor sensors increases. The average rate becomes stable when there are more than 10 indoor sensors.

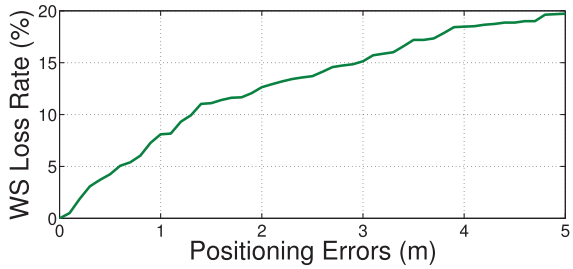

Fig. 10. Additional WS Loss rate (averaged) introduced by indoor positioning errors. The WISER prototype consists of 20 indoor sensors and one outdoor sensor.

7.4 Impact of Indoor Positioning Errors

Previous experiments show that WISER has good performance if indoor positioning is accurate. In practice, indoor positioning may incur errors. Therefore, it is important to evaluate the performance of our WISER prototype in the presence of indoor positioning errors.

Ideally, WISER returns the accurate indoor WS information at the user's position that is determined by the indoor positioning system without any false alarms. However, due to positioning errors, the user could appear anywhere within the circle that is centered at the reported position with a radius of a certain positioning error (in meters). Positioning errors are problematic, as they can manifest themselves in terms of both white space loss and (even worse) false alarms. To avoid false alarms, WISER returns the commonly available channels within the circle, which would result in an additional loss of white spaces. In this way, indoor positioning errors will not result in additional false alarms. To quantify the impact of positioning errors, we compute WS Loss rates of WISER with and without positioning errors, respectively, and measure this additional loss against the positioning error. We show the average case for the 65 locations in Figure 10. Note that a positioning

error of 5m would incur an average of 20% additional WS loss. To ensure the efficiency of WISER, the indoor positioning system should incur positioning errors less than a couple of meters.

8 CONCLUSIONS AND FUTURE WORK

White spaces promise to provide additional spectrum for wireless applications. However, the current rulings in the U.S. and Canada (and being considered elsewhere) adopt the geo-location database approach to determine spectrum availability, which works reasonably well but has limitations in both outdoor and indoor scenarios.

In this article, we carry out a measurement-driven approach to explore white space networking potential in Hong Kong, with the focus on indoor environments. We show that the indoor white spaces have different characteristics from the outdoor ones. For example, there are more contiguous unutilized TV channels indoors, which are able to support high-bandwidth communication. We then develop a system, called WISER, that is able to utilize the additional white space channels without requiring the clients to actually sense the wireless medium, by leveraging the power of clustering algorithms. We finally propose two effective algorithms to implement the system, of which the experimental results show that our system achieves much better performance than other baseline approaches. Any interested building can adopt our techniques to make the building "white space enhanced" and utilize the additionally available vacant TV channels.

There are several interesting and important future directions that could be explored. First, it would be very interesting to extend our two-dimensional system design, deployment, and experiments to three-dimensional (i.e., from one floor to multiple floors in the building) by jointly exploring channel, location, and space correlations. Second, it is also important to evaluate WISER's performance on different test-beds (e.g., halls, residential buildings) other than office buildings.

ACKNOWLEDGMENTS

We thank Wei Zhang for his help with clustering analysis. We also thank the anonymous reviewers and our shepherd of ACM Mobicom 2013 for giving insightful comments on the conference version of this article.

REFERENCES

Andreas Achtzehn et al. 2012. Improving coverage prediction for primary multi-transmitter networks operating in the TV whitespaces. In *Proceedings of the 9th Annual IEEE Communications Society Conference on Sensor, Mesh and Ad Hoc Communications and Networks (SECON'12)*. IEEE.

Andreas Achtzehn et al. 2014. Improving accuracy for TVWS geolocation databases: Results from measurement-driven estimation approaches. In *Proceedings of the IEEE International Symposium on Dynamic Spectrum Access Networks (DYSPAN'14)*. IEEE, 392–403.

Ari Asp et al. 2014. Impact of modern construction materials on radio signal propagation: Practical measurements and network planning aspects. In *Proceedings of the Vehicular Technology Conference (VTC'14)*. 1–7.

L. Bedogni, M. Di Felice, F. Malabocchia, and L. Bononi. 2014. Indoor communication over TV gray spaces based on spectrum measurements. In *Proceedings of the 2014 IEEE Wireless Communications and Networking Conference (WCNC'14)*. 3218–3223. DOI: http://dx.doi.org/10.1109/WCNC.2014.6953057

James C. Bezdek. 1981. *Pattern Recognition with Fuzzy Objective Function Algorithms*. Kluwer Academic Publishers, Norwell, MA.

CEDB. 2016. Location of the Digital Terrestial Television (DTT) Stations and the Estimated Coverage in Hong Kong. Retrieved from http://www.digitaltv.gov.hk/general/pdf/coverage.pdf (2016).

Vikram Chandrasekhar, Jeffrey G. Andrews, and Alan Gatherer. 2008. Femtocell networks: A survey. *IEEE Commun. Mag.* (2008).

X. Chen and J. Huang. 2013. Database-assisted distributed spectrum sharing. *IEEE J. Select. Areas Commun.* 31, 11 (November 2013), 2349–2361. DOI: http://dx.doi.org/10.1109/JSAC.2013.131110.

GNU Radio Community. 2016. GNU Radio. Retrieved from http://gnuradio.org/redmine/projects/gnuradio/wiki (2016).

ETTUS. 2016. Universal Software Radio Peripheral. Retrieved from http://www.ettus.com (2016).

Mauro Fadda, Vlad Popescu, Maurizio Murroni, Pablo Angueira, and Javier Morgade. 2015. On the feasibility of unlicensed communications in the TV white space: Field measurements in the UHF band. *Int. J. Dig. Multimed. Broadcast.* 2015 (2015).

FCC. Sep 2010. In the matter of unlicensed operation in the TV broadcast bands: Second memorandum opinion and order. FCC Std. 10-174 (Sep 2010).

Xiaojun Feng, Jin Zhang, and Qian Zhang. 2011. Database-assisted multi-ap network on TV white spaces: Architecture, spectrum allocation and ap discovery. In *Proceedings of the IEEE Symposium on New Frontiers in Dynamic Spectrum Access Networks (DySPAN'11)*. IEEE, 265–276.

C. Fraley and A. E. Raftery. 1998. How many clusters? Which clustering method? Answers via model-based cluster analysis. *Comput. J.* 41, 8 (1998), 578–588. DOI: http://dx.doi.org/10.1093/comjnl/41.8.578.

Mark Gibson. 2010. TV White Space Geolocation Database. Retrieved from http://ieee802.org/19/pub/Workshop/5_Gibson-ComSearch.pdf (2010).

Y. Gu, A. Lo, and I. Niemegeers. 2009. A survey of indoor positioning systems for wireless personal networks. *IEEE Commun. Surv. Tutor.* 11, 1 (quarter 2009), 13–32. DOI: http://dx.doi.org/10.1109/SURV.2009.090103

Kate Harrison, Shridhar Mubaraq Mishra, and Anant Sahai. 2010. How much white-space capacity is there? In *Proceedings of the IEEE Symposium on New Frontiers in Dynamic Spectrum (DySPAN'10)*. IEEE, 1–10.

Farzad Hessar and Sumit Roy. 2015. Capacity considerations for secondary networks in tv white space. *IEEE Trans. Mobile Comput.* 14, 9 (2015), 1780–1793.

Hong Kong Government HKGov. 2017. Hong Kong District Council. Retrieved from http://www.districtcouncils.gov.hk/index.html (2017).

O. Holland et al. 2015. To white space or not to white space: That is the trial within the Ofcom TV white spaces pilot. *Proceedings of the IEEE International Symposium on Dynamic Spectrum Access Networks (DySPAN'15)*. 11–22.

Md Habibul Islam, Choo Leng Koh, et al. 2008. Spectrum survey in singapore: Occupancy measurements and analyses. In *Proceedings of the 3rd International Conference on Cognitive Radio Oriented Wireless Networks and Communications (CrownCom'08)*. IEEE, 1–7.

P. Jallon. 2008. An algorithm for detection of DVB-T signals based on their second-order statistics. *EURASIP J. Wire. Commun. Netw.* 2008 (2008), 28.

J. Jr. 1963. Hierarchical grouping to optimize an objective function. *J. Am. Stat. Assoc.* 58, 301 (1963), 236–244.

N. Klepeis, W. Nelson, and W. Ott. 2001. The national human activity pattern survey (NHAPS): A resource for assessing exposure to environmental pollutants. *J. Expos. Anal. Environ. Epidemiol.* 11 (2001), 231–252. Issue 3. DOI: http://dx.doi.org/10.1007/BF01908075

Adrian Kliks et al. 2014. TVWS indoor measurements for HetNets. In *Proceedings of the Wireless Communications and Networking Conference Workshops (WCNCW'14)*. IEEE, 76–81.

Christoph König et al. 2014. Distributed indoor spectrum occupancy measurements in the UHF TV band. In *Proceedinsg of the 2014 IEEE International Conference on Communications (ICC'14)*. IEEE.

Dongxin Liu, Fan Wu, Linghe Kong, Shaojie Tang, Yuan Luo, and Guihai Chen. 2016. Training-free indoor white space exploration. *IEEE J. Select. Areas Commun.* 34, 10 (2016), 2589–2604.

D. Makris, G. Gardikis, and A. Kourtis. 2012. Quantifying TV white space capacity: A geolocation-based approach. In *IEEE Communications Magazine: Topics in Radio Communications*. IEEE.

M. McHenry, P. Tenhula, D. McCloskey, D. Roberson, and C. Hood. 2006. Chicago spectrum occupancy measurements & analysis and a long-term studies proposal. In *Proceedings of the 1st International Workshop on Technology and Policy for Accessing Spectrum*. ACM.

Elena Meshkova et al. 2013. Indoor coverage estimation from unreliable measurements using spatial statistics. In *Proceedings of the 16th ACM International Conference on Modeling, Analysis & Simulation of Wireless and Mobile Systems*. ACM.

Rohan Murty, Ranveer Chandra, Thomas Moscibroda, and Paramvir Bahl. 2012. Senseless: A database-driven white spaces network. *IEEE Trans. Mobile Comput.* 11, 2 (2012), 189–203.

OFCA. 2012. *Hong Kong Table of Freqency Allocaitons*. Technical Report. OFCA.

OFCA. 2016a. Hong Kong Digital Terrestrial TV Coverage & Reception Database. Retrieved from http://app1.ofca.gov.hk/apps/ubs/map.asp (2016).

OFCA. 2016b. Television Broadcasting Network of Hong Kong. Retrieved from http://www.ofca.gov.hk/filemanager/ofca/common/industry/broadcasting/television/free_tv/tvbnet.pdf (2016).

Alexandros Palaios, Janne Riihijärvi, and Petri Mähönen. 2014. From Paris to London: Comparative analysis of licensed spectrum use in two European metropolises. In *Proceedings of the IEEE International Symposium on Dynamic Spectrum Access Networks (DySPAN'14)*. IEEE, 48–59.

Caleb Phillips et al. 2012. Practical radio environment mapping with geostatistics. In *Proceedings of the IEEE International Symposium on Dynamic Spectrum Access Networks (DySPAN'12)*. IEEE, 422–433.

David Plets et al. 2009. Extensive penetration loss measurements and models for different building types for DVB-H in the UHF band. In *IEEE Trans. Broadcast.* Vol. 55. 213–222.

W. M. Rand. 1971. Objective criteria for the evaluation of clustering methods. *J. Am. Stat. Assoc.* 66, 336 (1971), 846–850. DOI: http://dx.doi.org/10.1080/01621459.1971.10482356

Tanim M. Taher, Roger B. Bacchus, Kenneth J. Zdunek, and Dennis A. Roberson. 2011. Long-term spectral occupancy findings in Chicago. In *Proceedings of the IEEE Symposium on New Frontiers in Dynamic Spectrum Access Networks (DySPAN'11).* IEEE.

Matthias Wellens et al. 2007. Evaluation of spectrum occupancy in indoor and outdoor scenario in the context of cognitive radio. In *Proceedings of the 2007 2nd International Conference on Cognitive Radio Oriented Wireless Networks and Communications.* IEEE.

Rui Xu and D. Wunsch II. 2005. Survey of clustering algorithms. *IEEE Trans. Neural Netw.* 16, 3 (May 2005).

L. Yan and M. Chen. 2011. *Exploring White Spaces in Metropolises: A Measurement Study in Hong Kong.* Technical Report. The Chinese University of Hong Kong. Retrieved from http://www.ie.cuhk.edu.hk/~mhchen/papers/HK.measurement.2011.pdf.

Sixing Yin, Dawei Chen, Qian Zhang, Mingyan Liu, and Shufang Li. 2012. Mining spectrum usage data: A large-scale spectrum measurement study. *IEEE Trans. Mobile Comput.* 11, 6 (2012), 1033–1046.

Xuhang Ying et al. 2015a. Revisiting TV coverage estimation with measurement-based statistical interpolation. In *Proceedings of the 7th International Conference on Communication Systems and Networks (COMSNETS'15).* IEEE.

Xuhang Ying, Sumit Roy, and Radha Poovendran. 2015b. Incentivizing crowdsourcing for radio environment mapping with statistical interpolation. In *2015 IEEE International Symposium on Dynamic Spectrum Access Networks (DySPAN'15).* IEEE.

Xuhang Ying, Jincheng Zhang, Lichao Yan, Guanglin Zhang, Minghua Chen, and Ranveer Chandra. 2013. Exploring indoor white spaces in metropolises. In *Proceedings of the 19th Annual International Conference on Mobile Computing & Networking.* ACM, 255–266.

Xuhang Ying, Sumit Roy, and Radha Poovendran. 2017. Pricing mechanisms for crowd-sensed spatial-statistics-based radio mapping. *IEEE Transactions on Cognitive Communications and Networking* 3, 2 (2017), 242–254.

J. Zhang, W. Zhang, M. Chen, and Z. Wang. 2015. WINET: Indoor white space network design. In *Proceedings of the IEEE Conference on Computer Communications (INFOCOM'15).* 630–638. DOI: http://dx.doi.org/10.1109/INFOCOM.2015.7218431.

Tan Zhang, Ning Leng, and Suman Banerjee. 2014. A vehicle-based measurement framework for enhancing whitespace spectrum databases. In *Proceedings of the 20th Annual International Conference on Mobile Computing and Networking.* ACM, 17–28.

Received November 2016; revised February 2017; accepted March 2017